Neurobiology of Aging xx (2012) xxx

A simultaneous ERP/fMRI investigation of the P300 aging effect

Redmond G. O'Connell[a,*], Joshua H. Balsters[a], Sophia M. Kilcullen[a], William Campbell[a], Arun W. Bokde[a], Robert Lai[b], Neil Upton[b], Ian H. Robertson[a]

[a] *Trinity College Institute of Neuroscience, Trinity College Dublin, Dublin, Ireland*
[b] *Neurosciences Centre of Excellence for Drug Discovery, GlaxoSmithKline, Harlow, UK*

Received 29 March 2011; received in revised form 16 December 2011; accepted 19 December 2011

Abstract

One of the most reliable psychophysiological markers of aging is a linear decrease in the amplitude of the P300 potential, accompanied by a more frontal topographical orientation, but the precise neural origins of these differences have yet to be explored. We acquired simultaneous electroencephalogram (EEG)/functional magnetic resonance imaging (fMRI) recordings from 14 older and 15 younger adults who performed a 3-stimulus visual oddball task designed to elicit P3a and P3b components. As in previous reports, older adults had significantly reduced P3a/P3b amplitudes over parietal electrodes but larger amplitudes over frontal scalp with no between-group differences in accuracy or reaction time. Electroencephalogram/functional magnetic resonance imaging fusion revealed that the P3a age effects were driven by increased activation of left inferior frontal and cingulate cortex and decreased activation of inferior parietal cortex in the older group. P3b differences were driven by increased activation of left temporal regions, right hippocampus, and right dorsolateral prefrontal cortex in the older group. Our results support the proposal that the age-related P300 anterior shift arises from an increased reliance on prefrontal structures to support target and distractor processing.

Keywords: P300; Aging; EEG; fMRI; Frontal; Target processing; Distractor processing

1. Introduction

The P300 event-related potential (ERP) has been 1 of the most extensively investigated human electrophysiological markers and has attracted interest from many researchers for its sensitivity to normal aging and age-related pathology (Friedman, 2003; Polich and Criado, 2006; Rossini et al., 2007; Sutton et al., 1965). In fact, P300 is an umbrella term that encompasses at least 2 functionally distinct subcomponents, P3a and P3b, each of which is elicited by a change in the stimulus environment and indexes separate attentional processes. The P3b has a parietal scalp distribution and is typically elicited 300–600 ms after the appearance of a rare target within a train of frequent irrelevant stimuli and, although its precise functional origins remain controversial, is taken to reflect the top-down allocation of attentional resources to stimulus evaluation (Donchin, 1981; Nieuwenhuis et al., 2005; Polich, 2007; Verleger, 2008). The P3a has a slightly earlier latency and a more anterior distribution than the P3b and is elicited by repeated deviant nontarget stimuli (as opposed to the fronto-central novelty P3 which is elicited by novel nonrepeating distractors). The P3a is proposed to reflect stimulus-driven, or bottom-up, attentional orienting to a salient but irrelevant stimulus (Polich, 2007; Richardson et al., 2011; Snyder and Hillyard, 1976). A number of studies have highlighted that the P300s provide useful biomarkers for normal aging and dementia (see Friedman, 2003; Rossini et al., 2007 for reviews) but our knowledge of the intracranial origins of the observed age-related changes remains limited. In the present study, we conduct the first simultaneous electroencephalogram (EEG)/functional magnetic resonance imaging (fMRI) exploration of age-related P300 effects.

Studies with large normative samples spanning the lifespan show that the amplitudes of the P3a and P3b decrease,

* Corresponding author at: Trinity College Institute of Neuroscience, Trinity College Dublin, Dublin 2, Ireland. Tel.: +353 1 896 8405; fax: 00 353 1 896318.
E-mail address: reoconne@tcd.ie (R.G. O'Connell).

and their peak latencies increase, linearly from adolescence through to senescence (Fjell and Walhovd, 2004; Polich, 1997). In addition, the aging process is reliably associated with a marked anterior shift in the topography of both components that is apparent across a range of different tasks (Fabiani et al., 1998; Friedman, 2003; Richardson et al., 2011; West et al., 2010). This increasingly frontal orientation appears to mirror 1 of the most consistently observed phenomena in neuroimaging investigations of aging; the greater recruitment of prefrontal regions and reduced activation of posterior regions that older subjects exhibit on a range of cognitive tasks (e.g., Cabeza et al., 2002; Davis et al., 2008; Solbakk et al., 2008). Because elderly participants are typically found to perform the oddball task at a comparable level with younger participants, the differences in P300 topography have been proposed to represent the compensatory activation of additional neural networks. Fabiani et al. (1998) explored this issue by dividing their elderly participant group according to those individuals who exhibited a frontal versus parietal P3b maximum. The "frontal" subgroup was found to perform significantly worse on standardized neuropsychological tests of frontal lobe function. This finding suggests that increased activation of prefrontal regions to support performance of simple target detection tasks is an inefficient processing method. More recently, studies by Richardson et al. (2011) and West et al. (2010) have provided evidence that the increased frontal focus of the P3a and P3b in elderly participants arises from a failure to habituate to the novelty of oddball stimuli. That is, because elderly participants are less able to establish a strong mental representation of task stimuli they continue to exhibit a novelty response to targets over frontal electrodes. This novelty response is also visible in young participants in the early stages of task performance but is gradually extinguished with increasing exposure to task stimuli. In support of the findings of Fabiani et al. (1998); West et al. (2010) also reported that increased frontal P300 amplitude was associated with worse performance on neuropsychological tests of executive function.

A significant limitation of this P300 work is that the intracranial generators of EEG activity cannot be reliably inferred on the basis of topographical distribution alone due to volume conduction and the inverse problem. Thus, the true source of the age-related frontal shift cannot be determined without recourse to other brain imaging methods. Another concern is that the findings from P300 studies are not easily reconciled with some of the evidence garnered from fMRI. For example, at least 1 fMRI study that employed a paradigm frequently used to elicit the P300 (oddball task), reported comparable prefrontal activation in young versus old participants (Madden et al., 2004). In addition, where the ERP studies mentioned above reported that greater frontal P300 amplitudes were associated with diminished prefrontal function in elderly subjects, Davis et al. (2008) found that increased blood oxygen level-dependent (BOLD) response in prefrontal regions was associated with better performance on a range of executive tasks. Consequently, an exploration of the precise neural source of age-related P300 differences is warranted to gain a more complete understanding of the effects of age on target and distractor processing.

The neural generators of the P300 have already been heavily investigated through lesion studies, depth electrode recordings, EEG source modeling algorithms, and functional neuroimaging (e.g., Bledowski et al., 2004; Halgren et al., 1995; Kiehl et al., 2001; Strobel et al., 2008). Although the results emerging from these different methodologies have been somewhat inconsistent and difficult to integrate, it has been established that P3a and P3b arise from widely distributed, partially overlapping frontotemporoparietal networks consistent with the proposal that they index distinct but related attention systems (Linden, 2005).

The fusion of EEG and fMRI data holds great promise in this regard. EEG traces cortical neural activity with fine-grained temporal accuracy (in the order of milliseconds) but allows only limited inferences to be drawn regarding underlying generators, especially when multiple generators are simultaneously activated. In direct contrast, fMRI provides a sophisticated structural and functional brain map but with limited temporal resolution due to the sluggish nature of the hemodynamic response. Because EEG and fMRI share a common neural source (local field potentials; Logothetis et al., 2001), the 2 methods can complement each other to provide spatial and temporal mapping of unparalleled resolution. A small number of EEG/fMRI data fusion studies with normal adults have already highlighted P300 networks (Bledowski et al., 2004; Eichele et al., 2005; Karch et al., 2010; Mantini et al., 2009; Strobel et al., 2008; Warbrick et al., 2009) that are broadly consistent with those reported with unimodal brain imaging and direct intracranial recordings, but this technique has yet to be applied to the study of cognitive aging.

EEG/fMRI data fusion methods have developed rapidly in the last 10 years and several different approaches to multimodal integration have been reported. In the present study we opt for an EEG-informed fMRI model which uses the variability of single-trial P3a/P3b amplitude as a predictor for the hemodynamic response to stimuli in a 3-stimulus visual oddball task (see Eichele et al., 2005; Novitskiy et al., 2011 for examples). These shifts occur on a time scale that can be sampled by fMRI, hence this kind of analysis is specialized to maximize the benefit of simultaneous acquisition by extracting single-trial information that is common to both modalities and that would otherwise be lost during standard averaging. When a consistent relationship is detected using this method one can infer that the corresponding fMRI activation either directly represents the source of P300 activity or contributes indirectly to that signal by modulating the direct generators. Age-related differences can then be highlighted by contrasting these activation maps between young and old groups. For comparison, we also conducted separate fMRI and EEG analyses using conventional analysis methods. In line with previous neuroim-

aging investigations, we predicted that age-related differences in these electrocortical components would be linked to increased activation of prefrontal cortex and diminished activity in posterior cortex.

2. Methods

2.1. Subjects

Sixteen young and 19 elderly neurologically normal, right-handed subjects participated in this study. One young participant and 5 elderly participants were not included in the analyses. Four of the elderly participants were removed due to poor EEG data quality (less than 20 trials accepted). One young and 1 elderly participant were removed for poor target detection accuracy (d-prime < 1). This left a final sample of 15 young and 14 elderly participants that were matched for gender, handedness, years of education, Hospital Anxiety and Depression Scale (HADS) score and Mini Mental State Examination (MMSE) score (Table 1). Participants gave written informed consent prior to the study which was approved by the Trinity College Dublin School of Psychology Ethics Committee.

2.2. Procedure

2.2.1. Visual oddball task

Participants performed a 3-stimulus visual oddball task (see Supplementary Fig. 1). Every 2075 ms a stimulus appeared on the screen for 75 ms. Standard stimuli consisted of a 3.5-cm diameter purple circle and appeared on 80% of trials. Target stimuli were a slightly larger purple circle (4 cm diameter) and appeared on 10% of trials. Distractor stimuli were a black and white checkerboard and appeared on 10% of trials. Participants were asked to make a speeded response to target stimuli using the response box placed in their right hand. The stimulus array was pseudorandomly designed such that between 3 and 5 standard stimuli were presented after any target or distractor stimulus. Thus, the minimum interval between a P3-eliciting event was 8300 ms but because targets and distractors were randomly interspersed throughout the task the interval between 2 targets or between 2 distractors could be as high as 64 seconds. The average was approximately 20 seconds, and approximately 70% of trials occurred between 8 and 22 seconds. All stimuli were presented on a gray background and participants were asked to maintain fixation on a white cross presented at the center of the screen. Participants performed 3 blocks inside the magnetic resonance imaging (MRI) scanner and each block consisted of 205 trials, including 20 targets and 20 distractors. Before entering the scanner, participants practiced the task in a dimly lit testing suite and performed 1 full block concurrent to EEG recording for signal-to-noise comparisons with EEG data acquired inside the scanner.

Table 1
Demographic information and oddball performance data

	Young	Old	t	p
Age (y)	22 (3.3)	70.6 (4.2)		
Gender	5/15 female	7/14 female	1.2	ns
Years of education	16.5 (2.9)	15.1 (2.8)	1.3	ns
HADS anxiety	4.2 (2.2)	3.5 (2.9)	0.7	ns
HADS depression	1.4 (1.7)	2.1 (1.9)	1.1	ns
MMSE	29.2 (0.9)	28.5 (1.2)	1.6	ns
Oddball performance				
Targets	41.4 (10.6)	49.1 (8.1)	2.2	<0.05
False alarm (%)	8.6 (12.3)	1.9 (1.9)	2.1	<0.05
D-prime	2.7 (0.6)	2.9 (1.2)	0.4	ns
RT	580.8 (85.5)	601.1 (125.5)	0.5	ns
RT variability	130.4 (40.5)	148.4 (51.4)	1.1	ns

Key: HADS, Hospital Anxiety and Depression Scale; MMSE, Mini Mental State Examination; ns, not significant; RT, . Data in parentheses represent standard deviation.

2.2.3. EEG-fMRI acquisition

Subjects lay supine in an MRI scanner with the thumb of the right hand positioned on a 2-button MRI-compatible response box. Stimuli were projected onto a screen behind the subject and viewed in a mirror positioned above the subject's face. Stimuli were presented using Presentation software (Version 15; Neurobehavioral Systems, Inc., Albany, CA, USA). EEG recordings were acquired with a 32-channel magnetic resonance (MR)-compatible BrainAmp system (Brainproducts, Munich, Germany). Thirty-three EEG electrodes were placed on the scalp, including the reference electrode positioned at FCz and the ground electrode placed at position AFz. One external electrode was applied to the subjects back in order to acquire the electrocardiogram (ECG) reading. Electrode impedances were maintained below 10 kΩ. The resolution and dynamic range of the EEG acquisition system were 100 nV and ± 3.2 mV, respectively. Data were recorded on a laptop computer through Brain Recorder v1.04 software (BrainProducts, Munich, Germany) at a sampling rate of 5 kHz with a band-pass filter of 0.016 to 250 Hz. Event timings, response timings, and transistor-transistor logic (TTL) pulses from the MRI scanner at the onset of each volume acquisition were marked within the EEG trace. The TTL pulses were also used to drive the visual stimuli in Presentation (Neurobehavioral Systems, Inc.). The EEG clock was synchronized to the MRI scanner clock using the Brainproducts Sync-box (Munich, Germany) (Mullinger et al., 2008). Event timings and reaction times were calculated off-line using event timings acquired by Brain Recorder v1.04 software (BrainProducts) at this higher frequency sampling.

A high-resolution T1-weighted anatomic magnetization prepared rapid gradient echo (MPRAGE) image (field of view [FOV] = 230 mm, thickness = 0.9 mm, voxel size = 0.9 mm × 0.9 mm × 0.9 mm), as well as phase and magnitude maps were acquired first (echo time $[TE]_1$ = 1.46 ms, TE_2 = 7 ms). Each participant then performed 3 echo planar imaging (EPI) sessions, each containing 228 volumes. The field of view covered the whole brain, 224 mm × 224 mm (64 × 64 voxels), 34 axial slices were acquired (0.05 mm slice gap) with a voxel size of 3.5 mm ×

3.5 mm × 4 mm; time resolution (TR) = 2 seconds, TE = 32, flip angle = 78°. This was a sparse-sampling sequence with the slices compressed to the first 1700 ms of the TR, leaving 300 ms uncontaminated by the MR gradient artifact (Debener et al., 2005). Each EPI session lasted 8 minutes. All MRI data were collected on a Philips 3T Achieva MRI Scanner (Trinity College, Dublin, Philips, DA Best, Netherlands).

2.2.4. EEG preprocessing and analysis

EEG data were preprocessed using Analyser software, version 2.01 (BrainProducts). Before preprocessing, the first TTL pulse of each EPI session was removed as it occurred at a different point in the gradient artifact template. After this, gradient correction was applied using the average artifact subtraction (AAS) method (Allen et al., 2000), and a moving average of 25 windows. EEG data were then downsampled to 512 Hz and filtered between 0.53 and 30 Hz using Infinite Impulse Response filters with an additional 50 Hz notch filter. R-peaks were then detected in the electrocardiogram channel and removed using the average artifact subtraction method (Allen et al., 1998), and a moving average of 11 artifacts. For both the gradient and balistocardiogram (BCG) correction, multiple average window lengths were tested and the chosen values (25 windows for gradient correction, and 11 windows for BCG correction) were found to effect the maximal power decreases at contaminated frequencies. Independent components analysis (ICA) was then conducted on the whole data set to remove remaining artifacts including blinks, eye movements, electromyogram (EMG), and residual BCG artifacts based on visual inspection of component topographies and time courses (Debener et al., 2007, 2008). Standard trials (excluding false alarms), targets trials (excluding misses), and distractor trials (excluding false alarms) were epoched (−1000 ms to 1000 ms) separately and baseline corrected for the interval −200 to 0 ms. Single epochs that exceeded predetermined artifact thresholds (100 mV difference, ± 80 μV value, and 100-μV gradient, 5 × SD difference) were rejected and all data were rereferenced using an average reference.

For the conventional ERP analysis P3b amplitude was measured as the peak positive voltage in the window 300–600 ms following target onset in the averaged target waveforms of each individual from separate frontal (F3, Fz, F4), central (C3, Cz, C4), and parietal (P3, Pz, P4) electrode clusters. P3a amplitude was measured as the peak positive voltage in the window 300–600 ms following distractor onset using the same channels. In order to further explore between-group differences in ERP scalp distribution across the entire P3a/P3b time course we also performed statistical cluster analysis on the averaged target and distractor waveforms. This technique consists of calculating pointwise, independent samples (old vs. young), 2-tailed *t* tests separately for the P3a and P3b time windows (300–600 ms) for all midline scalp sites (FP1, FP2, F3, Fz, F4, FC1, FCz, FC2, C3, Cz, C4, CP1, CP2, P3, Pz, P4, O1, Oz, O2) and displayed the *p* values as a 2-dimensional statistical color-scaled map (see Dockree et al., 2005; Wylie et al., 2003 for other examples of this approach). Only *p* values of less than 0.05 are displayed in the statistical cluster plot.

To facilitate the EEG/fMRI analysis a wavelet denoising procedure was implemented to obtain reliable single-trial measures of P3 amplitude at electrodes Fz and Pz. The EP_den_v2 plug-in for MATLAB, version 2009a (Mathworks, Natick, MA, USA) (Quian Quiroga and Garcia, 2003) uses wavelet decomposition of the average ERP as a denoising template and applies the wavelet coefficients which are correlated with the ERP components of interest back to each single-trial. Wavelet denoising in this way has optimal resolution in both the frequency and time domains and allows the effective removal of extraneous noise from the single-trial waveforms.

Finally we also analyzed early visual components elicited by target and distractor trials using the average of electrodes O1 and O2. Both distractors and targets elicited a P1 which was measured as the peak positive voltage between 80 and 120 ms. Distractors elicited 2 additional components, the N1 and P2. N1 was measured as the maximum negative voltage between 150 and 180 ms and the P2 was measured as the peak positive voltage between 200 and 250 ms.

2.2.5. fMRI preprocessing and analysis

Scans were preprocessed using SPM8 (www.fil.ion.ucl.ac.uk/spm). Before preprocessing EPI data quality tests were conducted using the criterion defined in Iannetti et al. (2005). These include assessing the mean and standard deviation of the signal time course, image signal to noise, standard deviation of the single voxel signal time course, and visual inspection for ghost artifact and signal dropout. All EPI data collected passed these tests. Images were then realigned and unwarped using field maps to correct for motion artifacts, susceptibility artifacts and motion-by-susceptibility interactions (Andersson et al., 2001; Hutton et al., 2002). Images were subsequently normalized to the International Consortium for Brain Mapping (ICBM) EPI template using the unified segmentation approach (Ashburner and Friston, 2005). Lastly, a Gaussian kernel of 8 mm was applied to spatially smooth the image in order to conform to the Gaussian assumptions of a General-Linear Mode (GLM) as implemented in SPM8 (www.fil.ion.ucl.ac.uk/spm) (Friston et al., 1995a, 1995b).

Four event types were modeled at the first level (Standard, Target, Distractor, and Error). A GLM was constructed from regressors formed by the convolution of event delta functions with the Fourier basis set (Balsters and Ramnani, 2008). Target trials to which participants failed to respond, or Standard or Distractor stimuli with false alarms, were modeled separately as a fourth event type and were differentiated from events of experimental interest. Thus, activity time-locked to incorrect trials was excluded from the regressors of interest. The residual effects of head mo-

tion were modeled in the GLM by including the 6 head motion parameters acquired from the realignment stage of the preprocessing as covariates of no interest. Prior to the study, a set of planned experimental timings were carefully checked so that they resulted in an estimable GLM in which the statistical independence of the event types was preserved. A random effects analysis (2-way analysis of variance [ANOVA]: Group [Young, Elderly] by Basis Function [2 Sine, 2 Cosine, 1 Envelope]) was run to determine significant differences in voxels at a group level.

2.2.6. EEG-fMRI data fusion

Similar to previous studies, single trial ERP information was used to guide the fMRI analyses (Debener et al., 2005; Eichele et al., 2005; Warbrick et al., 2009). In order to further improve signal-to-noise ratios each wavelet-denoised single trial ERP was smoothed using the mean of the 2 adjacent trials and single trial P3a/P3b amplitudes were defined as the maximum absolute value between 300 and 600 ms. As a consequence of the smoothing step, the results reported below highlight relatively sustained or tonic variance in the fMRI and broad-band ERP measures. Given the additional frontal recruitment with aging, and the strong parietal focus of both the P3a and P3b ERP components (Fig. 1), values were extracted from electrodes Fz and Pz for both target and distractor ERPs.

As specified above (fMRI preprocessing and analysis) GLMs were constructed with 4 conditions of interest (Standard, Target, Distractor, and Error) and each of these conditions was modeled using 5 Fourier basis functions to account for variability in the hemodynamic response function between subjects (Aguirre et al., 1998; Handwerker et al., 2004) and between groups (D'Esposito et al., 2003; Kannurpatti et al., 2010). These regressors highlight the generic obligatory response to target and distractor stimuli of constant amplitude associated with "exogenous" features of the task such as primary visual processing and the motor response (see Eichele et al., 2005). For both Target and Distractor trials, additional regressors were included in the GLM encoding the single trial ERP amplitude recorded at a specific electrode (each Fourier basis function was parametrically modulated adding an extra 5 regressors per condition to the GLM). Separate GLMs were run for Fz and Pz single-trial amplitudes as these were found to be significantly correlated in Young participants. This also reduced the chance of false negatives due to inadequate degrees of freedom. Parametric modulators were decorrelated from the constant amplitude regressors (Schmidt-Gram orthogonalization), ensuring that any amplitude-modulated activation present was specific to the electrophysiological measure and not to some general feature in the evoked response to targets or distractors. A random effects analysis (2-way ANOVA: Group [Young, Elderly] by Basis Function [2 Sine, 2 Cosine, 1 Envelope]) was run to determine significant differences in voxels at a group level. ERP-fMRI results were thresholded at a lower level to fMRI only results consistent with the literature ($p < 0.001$ uncorrected, extent threshold 10 voxels [e.g., Ben-Simon et al., 2008; Debettencourt et al., 2011; Eichele et al., 2005; Karch et al., 2010; Novitskiy et al., 2011]).

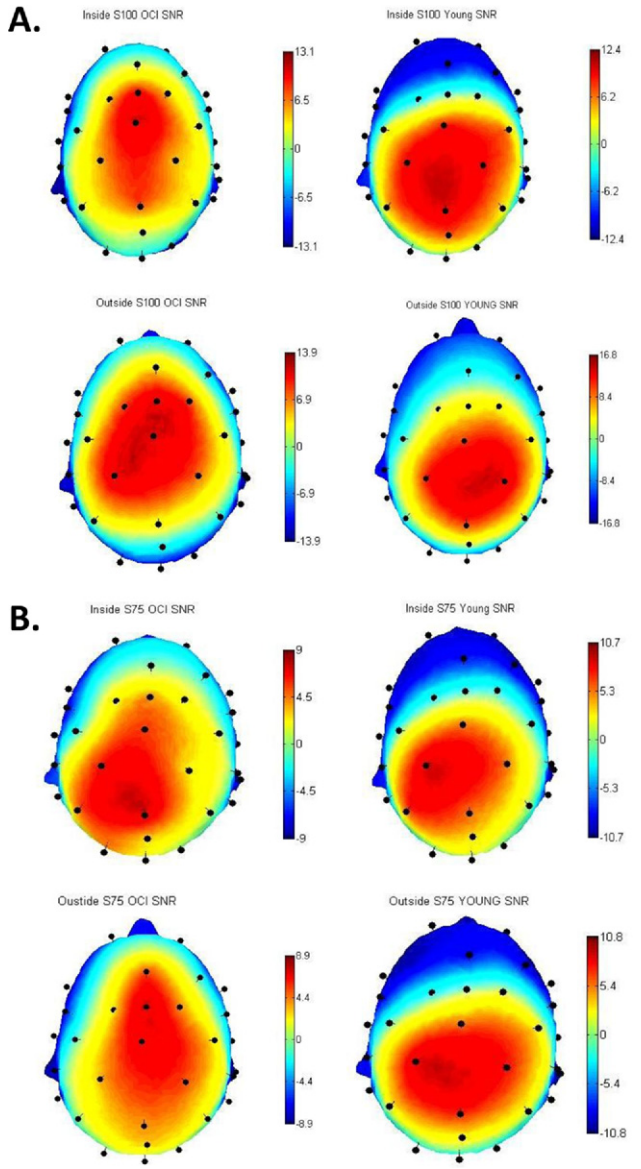

Fig. 1. (A) Signal-to-noise scalp topographies for the P3a collected inside and outside the MRI scanner. (B) Signal-to-noise scalp topographies for the P3b collected inside and outside the MRI scanner.

3. Results

3.1. Behavior

A full breakdown of the oddball performance scores is provided in Table 1. While elderly participants were significantly better at detecting target stimuli compared with young participants, $t(1,27) = 2.2$, $p < 0.05$, they also made

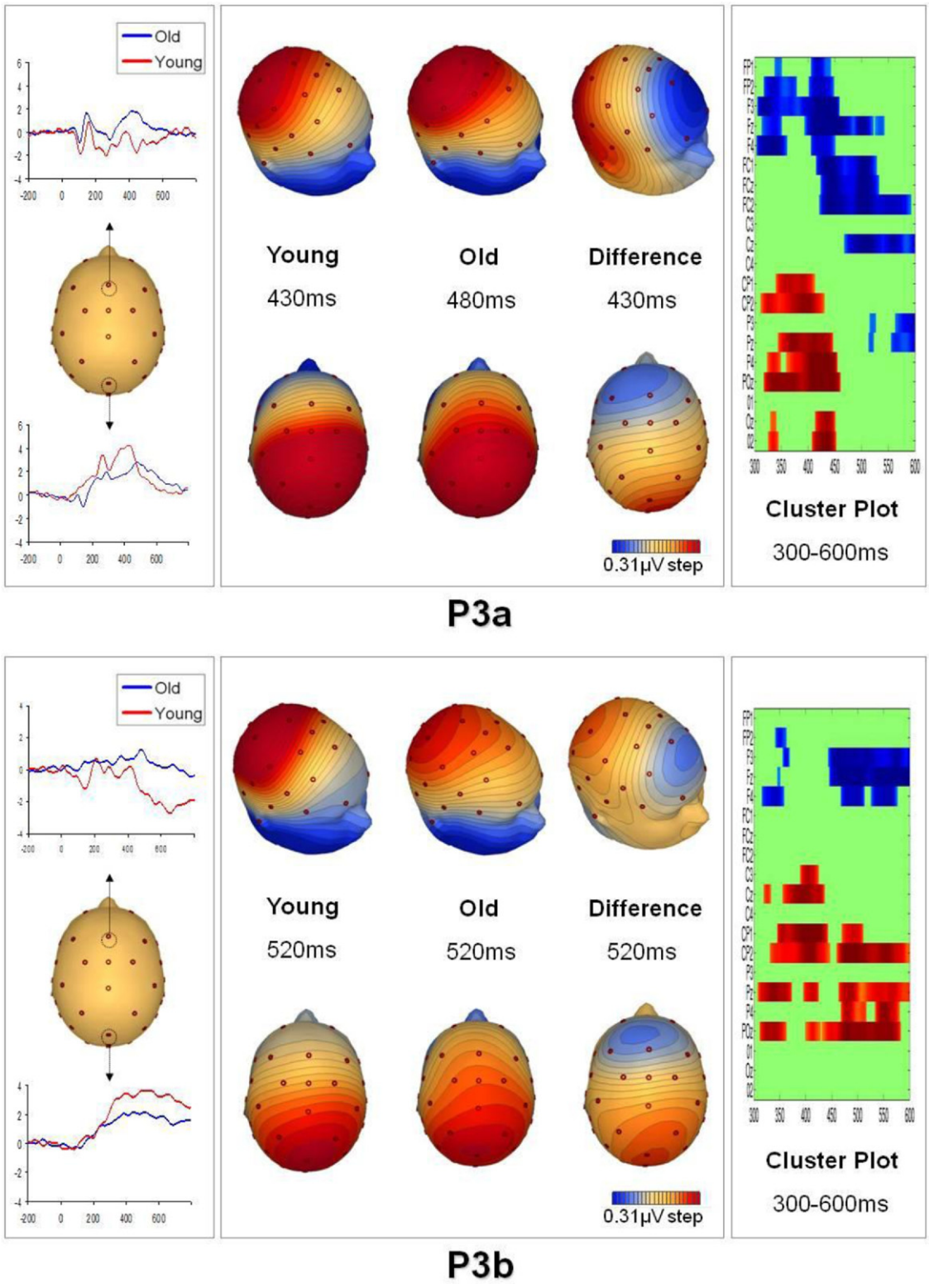

Fig. 2. Grand-average event-related potentials (left panels), scalp topographies (center panels) and statistical cluster plots (right panels) for P3a (top) and P3b (bottom). The young group had significantly larger P3a and P3b amplitudes relative to the old group. The scalp topographies and cluster plots highlight the significant age-related frontal shift that was observed for both components. For the difference topography and cluster plot, blue denotes old > young and red denotes young > old.

significantly more false alarms on standard trials, $t(1,27) = 2.1$, $p < 0.05$. Consequently, there were no significant differences in d-prime scores ($p = 0.7$) nor were there any significant differences in reaction time ($p = 0.6$), reaction time variability ($p = 0.3$), or false alarms to distractors ($p = 0.4$).

3.2. ERPs

Fig. 2 shows the grand average ERP waveforms, scalp topographies and statistical cluster maps for both the distractor (P3a) and target (P3b) trials and mean peak and peak latency values are provided in Table 2. As a quality control step we measured signal-to-noise ratios (peak poststimulus amplitude divided by root mean square of the baseline interval) for ERP data collected inside versus outside the scanner and found that there were no significant effects of location for targets or distractors (target: $p = 0.5$; distractor $p = 0.8$) and there were no group by scanner interactions (target: $p = 0.4$; distractor $p = 0.3$; see Fig. 1 and Supplementary data).

Age effects on the peak amplitudes and peak latencies of the P3a and P3b were first statistically analyzed using a 2-way ANOVA with factors of Group (Young vs. Elderly) and Region (Frontal, Central, and Parietal). For the P3a, there was a significant main effect of Region, $F(2,54) = 14.1$, $p < 0.001$, driven by significantly smaller amplitudes over Frontal compared with Central ($p < 0.001$) and Parietal ($p < 0.01$) scalp regions, and a significant Group by Region interaction, $F(2,54) = 6.54$, $p < 0.01$, arising from significantly larger amplitudes for young participants over Parietal scalp ($p < 0.05$). There was also a significant main effect of Group on P3a peak latency, $F(1,27) = 7.84$, $p < 0.01$, with elderly participants showing significantly later peak latencies.

For the P3b there was a significant main effect of Group, $F(1,27) = 5.51$, $p < 0.05$, with larger amplitudes overall in the young group and a significant main effect of Region, $F(2,54) = 18.54$, $p < 0.001$, driven by the significantly smaller amplitudes in Frontal compared with Central ($p < 0.001$) and Parietal ($p < 0.001$) regions. There was also a significant Group by Region interaction, $F(2,54) = 5.74$, $p < 0.01$, with significantly larger amplitudes in the young group over Central ($p < 0.05$), and Parietal ($p < 0.01$) scalp compared with the old group. There were no significant differences in P3b peak latency.

The statistical cluster plots confirmed the group differences in parietal P3a and P3b amplitudes but also clearly indicated that, although the frontal contrasts did not reach significance in the main ANOVA using the peak positive voltage measure, the elderly group did have consistently larger positive values over frontal scalp channels when taking in the entire P300 time course (300–600 ms) (see Fig. 1). Inspection of the grand-average ERP waveforms indicates that the frontal P3a differences were driven by a greater positive deflection in the old versus young group but the P3b differences arose from a substantial negative deflection in the young group that was not apparent in the old group.

Finally, the amplitudes of the earlier visual components, P1, N1, and P2 were also compared between groups on target and distractor trials (Fig. 3). The young group had significant larger P1 ($p < 0.01$) and P2 ($p < 0.01$) amplitudes compared with the old group but there were no significant differences in the amplitude of the N1.

3.3. fMRI-only analysis

fMRI data were analyzed using a 2-way ANOVA with factors of Group and Basis function. A statistical conjunction was run to find regions commonly active in both young and elderly participants. During target processing a common network of visual and motor regions were active including the supplementary motor area (SMA), left primary motor cortex, left insula, right inferior parietal cortex, and extrastriate cortex. During distractor processing only visual regions were commonly active (Table 3).

Significant between-group differences were also assessed in the fMRI data. A significant reduction in visual activity in Elderly participants for both distractor and target processing was observed. This was accompanied by significantly more activity within the left middle frontal gyrus (Brodmann area [BA] 44) and the right insula cortex for the processing of distractors and targets respectively. These same regions were highlighted in the analysis of the first regressors included in the EEG-fMRI model (i.e., generic obligatory response to targets and distractors, see Tables 4–6) suggesting that these activation differences related to exogenous, stimulus-evoked processes that did not relate to P3a/P3b.

3.4. EEG-fMRI

Given the anterior-posterior differences between groups highlighted in Fig. 2, single trial amplitudes were taken from electrodes Fz and Pz and used as separate parametric modulators. Having 2 ERP modulators allowed us to exclude global

Table 2
Mean peak and peak latency data for P3a and P3b components

	Site	Young ($n = 15$)	Old ($n = 14$)	t	p
P3a					
Peak	Frontal	1.59	2.54	1.49	ns
	Central	3.91	3.13	1.28	ns
	Parietal	4.51	3.03	2.47	<0.05
Latency	Frontal	405.02	432.33	1.17	ns
	Central	411.56	478.14	3.39	<0.005
	Parietal	405.38	466.90	2.83	<0.01
P3b					
Peak	Frontal	1.14	1.70	1.05	ns
	Central	3.50	2.18	2.73	<0.05
	Parietal	4.22	2.68	3.00	<0.01
Latency	Frontal	482.36	459.67	0.73	ns
	Central	468.40	477.86	0.42	ns
	Parietal	476.93	468.95	0.33	ns

Key: ns, not significant.

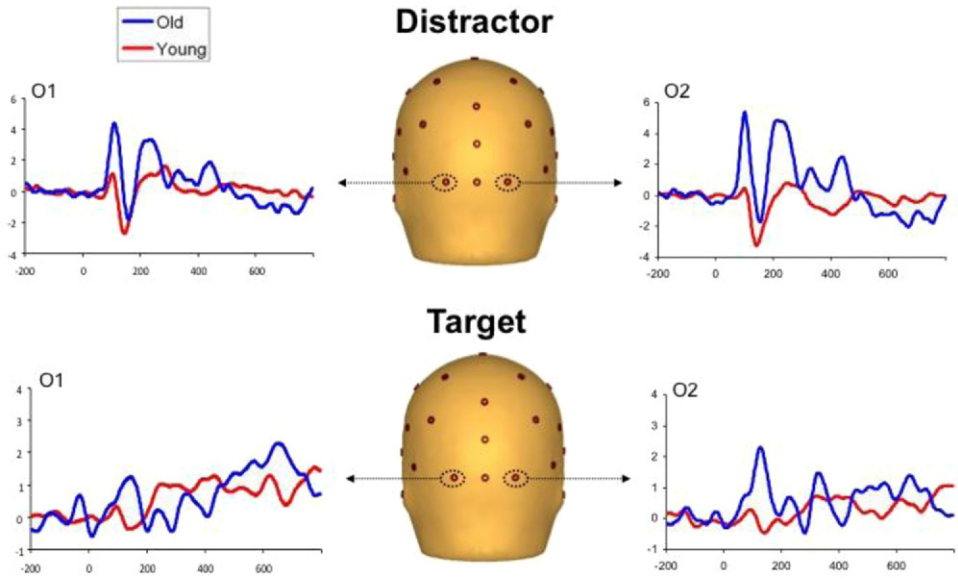

Fig. 3. Grand-average event-related potentials from bilateral occipital electrodes (O1/O2) highlighting early visual responses to distractors and targets. The elderly group had significantly smaller P1 and P2 amplitudes on distractor trials and significantly smaller P1 amplitudes on target trials.

EEG differences and focus on the fMRI correlates of specific regional ERP differences. Regional activations showing significant between-group effects are highlighted in Fig. 4 and are summarized in Tables 5 (P3a) and 6 (P3b).

3.4.1. P3b - electrode Fz

The elderly group showed increased correlation within the right middle frontal gyrus (BA 9), left putamen, and right hippocampus. Young participants showed increased correlations in the right orbitofrontal gyrus (BA 47).

3.4.2. P3b - electrode Pz

The elderly group showed increased correlation in the left superior temporal gyrus and prefrontal-projecting territories of the left cerebellar hemisphere (crus II). The young showed greater correlation in the left temporal pole and decreased correlation in the right hippocampus (FD).

3.4.3. P3a - electrode Fz

The elderly group showed greater correlations in the left inferior frontal gyrus (Pars Triangularis; BA 44), right middle cingulate cortex (BA 23), and right hippocampus. There were also relatively increased correlations in right intraparietal sulcus (hIP1) in the young group.

3.4.4. P3a - electrode Pz

The elderly group showed increased correlation within right putamen, and cerebellar vermis (I–IV) while the young group showed increased correlation within left insula.

4. Discussion

The goal of this study was to elucidate the intracranial origins of the commonly reported age-related P300 effects through spatiotemporal integration of simultaneously ac-

Table 3
fMRI-only conjunction results for distractor and target trials

	Brain area	Cluster size	*F*	Coordinates			Cytoarchitectonic BA (probability if available)
				x	y	z	
Distractor fMRI only							
$p < 0.05$, FWE-corrected	Lingual Gryus	2419	20.5	−8	−72	−6	hOC4v (50%), hOC3v (40%), area 17 (20%)
	Target fMRI only						
$p < 0.05$, FWE-corrected	Left insula	30	9.4	−30	16	2	Area 48
	Left SMA	17	9.1	−4	−2	52	Area 6 (80%)
	Left insula	35	10.4	−42	−4	4	Area 48
	Left postcentral gyrus	630	14.6	−48	−24	46	Area 2 (80%), area 1 (30%)
	Right inferior parietal lobule	68	9.2	46	−44	48	IPC (PFm) (60%), hIP3 (20%), hIP2 (20%)
	Right angular gyrus	30	9.7	34	−52	38	hIP3 (30%)
	Lingual gryus	655	11.4	10	−74	−6	Area 18 (40%), hOC3v (30%)
	Right superior occipital gyrus	25	8.8	22	−82	16	Area 19

Cluster size refers to number of voxels activated. Negative x coordinates refer to left hemisphere activations.
Key: BA, Brodmann area; fMRI, functional magnetic resonance imaging; FWE, family-wise error; hIP, human intraparietal area; SMA, supplementary motor area.

Table 4
fMRI-only between-group differences for distractor and target trials

	Brain area	Cluster size	*F*	Coordinates			Cytoarchitectonic BA (probability if available)	Group difference
				x	y	z		
Distractor fMRI only								
$p < 0.05$, FWE corrected	Calcarine gyrus	624	11.09	16	−60	6	Area 17 (80%)	Young decrease
	Left middle frontal gyrus	224	8.08	−28	10	34	Area 44	Elderly increase
Target fMRI only								
$p < 0.05$, FWE corrected	Lingual gyrus	816	8.4	12	−56	8	Area 17 (70%), area 18 (20%)	Young decrease
	Right insula	219	8.25	40	−4	14	Insula ld1 (80%)	Elderly increase

Cluster size refers to number of voxels activated. Negative x coordinates refer to left hemisphere activations. For most active group Young or Elderly refers to the group driving the effect, increase or decrease refers to the direction of the BOLD response.
Key: BA, Brodmann area; fMRI, functional magnetic resonance imaging; FWE, family-wise error; ld1, insula dysgranular.

quired EEG and fMRI data. In line with many previous studies conducted outside the scanner, we found that the older group exhibited diminished P3a and P3b amplitudes over parietal scalp sites and a significant frontal shift in the topography of both components. For the first time however, EEG/fMRI data fusion enabled us to observe the sources of these differences, highlighting increased recruitment of prefrontal and temporal regions and decreased recruitment of inferior parietal cortex in the older group. Our results lend support to the proposal that the P300 age-related frontal shift arises from an increased reliance on prefrontal structures to support target and distractor processing but also highlight a more complex pattern of additional regional activation differences.

The integration of EEG and fMRI data are still in relative infancy and a significant obstacle to progress has been resolving the substantial artifacts that are associated with collecting EEG in the scanner environment. Our analysis of signal-to-noise ratios for data collected inside versus outside the scanner clearly indicate that the gradient and BCG correction methods used here were successful and resulted in P300s that were comparable in morphology and amplitude. The conventional P3a/P3b analysis of data collected inside the scanner also produced results that are highly consistent with the extant aging literature. Over parietal scalp sites, the older group had significantly smaller peak amplitudes for both the P3a and P3b although latency differences only reached significance for the P3a. The statistical cluster analysis of scalp distribution confirmed that the older group had significantly smaller P3a/P3b amplitudes over parietal electrodes compared with the young group but also highlighted additional differences over frontal electrodes that did not reach significance using the conventional single peak measurement approach. The absence of significant frontal effects in the conventional analysis, despite clear numerical trends (see Table 2), is likely due to the relatively low participant numbers included in this study. The broader scope of the cluster analysis, which analyzes

Table 5
P3a-informed fMRI results

	Brain area	Cluster size	*F*	Coordinates			Cytoarchitectonic BA (probability if available)	Group difference
				x	y	z		
Distractor fMRI only								
$p < 0.05$, FWE corrected	Left middle frontal gyrus	215	8.3	−28	10	34	Area 44	Elderly increase
	Right calcarine gyrus	675	11.4	16	−60	6	Area 17 (80%)	Young decrease
Fz-P3a single trial								
$p < 0.001$, uncorrected; extent 10 voxels	Left inferior frontal gyrus (p. Triangularis)	14	4.8	−34	32	16	Area 44 (10%)	Elderly increase
	Left inferior frontal gyrus (p. Triangularis)	29	5.2	−36	18	24	Area 44 (30%)	Elderly increase
	Right middle cingulate cortex	16	5.9	14	−12	44	Area 23	Elderly increase
	Right hippocampus	10	4.9	26	−32	−10	Hipp (SUB) (70%), Hipp (CA) (70%)	Elderly increase
	Right intraparietal sulcus	10	4.9	34	−46	28	hIP1 (50%)	Young increase
Pz-P3a single trial								
$p < 0.001$, uncorrected; extent 10 voxels	Left insula	14	5.6	−42	−12	−10	Insula (IG2) (30%), Op3 (20%)	Young increase
	Cerebellar vermis	11	5.6	2	−48	−24	Lobule I–IV (hem) (47%)	Elderly increase
	Right putamen	67	7.7	34	8	−4	NA	Elderly decrease

Cluster size refers to number of voxels activated. Negative x coordinates refer to left hemisphere activations. For most active group Young or Elderly refers to the group driving the effect, increase or decrease refers to the direction of the BOLD response.
Key: BA, Brodmann area; CA, cornu ammonis; fMRI, functional magnetic resonance imaging; FWE, family-wise error; hem, ; hIP1, human intraparietal area; Hipp, hippocampus; IG, insular granular; NA, not applicable; Op, operculum; SUB, subiculum.

Table 6
P3b-informed fMRI results

	Brain area	Cluster size	*F*	Coordinates			Cytoarchitectonic BA (probability if available)	Group difference
				x	y	z		
Target fMRI only								
$p < 0.05$, FWE	Right insula lobe	214	8.3	40	−4	−14	Insula (ld1) (40%)	Elderly increase
corrected	Right lingual gyrus	928	8.4	12	−56	8	Area 17 (70%), area 18 (20%)	Young decrease
Fz-P3b single trial								
$p < 0.001$, uncorrected,	Right middle orbital gyrus	27	5.6	32	46	−2	Area 47	Young increase
extent 10 voxels	Right middle frontal gyrus	18	5.9	32	10	46	Area 9	Elderly increase
	Left putamen	22	5.5	−20	14	4	NA	Elderly increase
	Right hippocampus	26	5.7	28	−18	−6	Hipp (CA)	Elderly increase
Pz-P3b single trial								
$p < 0.001$, uncorrected,	Left temporal pole	27	5.6	−30	4	−26	Amyg (LB) (1.3%)	Young decrease
extent 10 voxels	Left superior temporal gyrus	22	5	−42	−4	−8	Area 48	Elderly increase
	Right hippocampus	11	5.2	26	−28	−6	Hipp (FD) (40%), Hipp (SUB) (20%)	Young decrease
	Left cerebellum	26	5.1	−16	−66	−36	Crus II	Elderly increase

Cluster size refers to number of voxels activated. Negative x coordinates refer to left hemisphere activations. For most active group Young or Elderly refers to the group driving the effect, increase or decrease refers to the direction of the BOLD response.
Key: Amyg, amygdala; BA, Brodmann area; BOLD, blood oxygen level-dependent; CA, cornu ammonis; FD, fascia dentate; fMRI, functional magnetic resonance imaging; FWE, family-wise error; Hipp, hippocampus; ld1, insula dysgranular; LB, latero-basal; NA, not applicable; SUB, subiculum.

every electrode and each time point within the P300 latency range made it possible to demonstrate both frontal and posterior age effects. These differences were observed despite the fact that the 2 groups did not differ in their reaction time or target detection accuracy (d-prime). In fact, the older group made significantly more correct responses to target stimuli but this was offset by a greater tendency to make false alarms on standard trials (see Richardson et al., 2011 for similar results). The absence of substantial performance differences suggests that the older group were relatively high functioning but this did not obscure the characteristic age-related electrocortical differences.

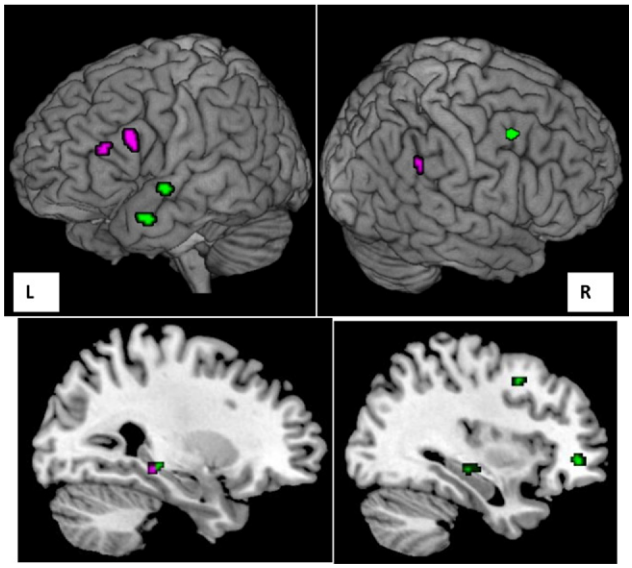

Fig. 4. P3a and P3b informed fMRI regional activation group differences. Pink denotes P3a-related differences and green denotes P3b-related differences. The top panel highlights differences on the lateral convexity of the cerebral cortex and the bottom panels show sagittal slices highlighting group differences within the hippocampus.

For the purposes of comparison we also conducted a conventional fMRI analysis that distinguished between target and distractor detection and isolated regional activations that were either common or specific to the 2 participant groups. The results are broadly consistent with previous neuroimaging investigations of the oddball task, highlighting a well-established target detection network that comprises occipital, inferior parietal/temporoparietal, and insular cortices (Linden, 2005) although no significant frontal activation was observed when collapsing across groups. It is noteworthy that target processing recruited a substantially more widespread network of regions in comparison with distractors for which only visual regions were significantly activated (see Bledowski et al., 2004; Kiehl et al., 2001 for similar examples). This difference likely reflects the passive nature of distractor processing while target detection depends on active attentional engagement and response execution. The conventional fMRI analysis also revealed additional regional activations that were group-specific. The elderly group exhibited significantly increased activity in the left middle frontal gyrus for distractors and in the right insular cortex during target processing but the EEG/fMRI fusion analysis indicated that these activations were related to obligatory, stimulus-evoked processes and not the P3a/P3b. This observation underlines the fact that, because the hemodynamic response occurs over a latency that comprises multiple information processing stages, fMRI activations cannot be reliably related to P300 age effects without conducting multimodal analyses. The enhanced temporal accuracy provided by the integration of ERP information allowed us to uncover age-specific fMRI modulations that were not observable following a conventional analysis.

In the present study we adopted an EEG/fMRI fusion analysis in which the amplitude of the P3a and P3b were used as regressors in an EEG-informed fMRI analysis that specifically isolated regional activations that differed between the young and old groups. In order to improve the stability of these results, each single-trial ERP was smoothed by averaging it with the 2 adjacent trials. Given that the average intertarget interval was 20 seconds these fusion results therefore represent shared fMRI and ERP modulations that manifest over a relatively broad time scale. The P3b-informed analysis revealed age-related activation differences in several regions of the well-characterized target detection/P3b network with the elderly group showing significantly increased activation in the right dorsolateral prefrontal cortex, left superior temporal cortex, and left cerebellum. The young participants showed significantly less activity in these areas and also exhibited activation decreases in the left temporal pole and right hippocampus. The only brain region in which young participants showed greater P3b activity was the right orbitofrontal gyrus. The P3a-informed analysis followed a similar pattern highlighting multiple activation increases for the elderly group in left inferior frontal cortex, right cingulate cortex, and the cerebellar vermis, and a decreased activation of right inferior parietal cortex relative to the young group—regions that have been previously implicated in distractor processing.

The aging brain undergoes gradual widespread decreases in gray matter volume and degeneration of white matter structures and neuroimaging studies have shown that the prefrontal cortex is 1 of the regions that undergoes the largest volumetric reductions (Raz, 2000; Raz et al., 2005). In tandem with these neural changes, cognitive functions that depend on the integrity of the frontal lobes, such as working memory, inhibitory control, and attention, are particularly vulnerable to age-related decline while other abilities, such as short-term memory, are relatively spared (Goh and Park, 2009; Gunning-Dixon and Raz, 2003; Raz, 2000). At the same time, functional neuroimaging studies have paradoxically reported consistent age-related increases in the magnitude and spatial extent of activity within prefrontal cortex (e.g., Cabeza et al., 2002; Davis et al., 2008; Solbakk et al., 2008). In younger adults, the activity in high-level control areas gradually decreases after a task has been well rehearsed and further processing is largely delegated to task specific brain regions (Kelly and Garavan, 2005). It has been proposed that the continued engagement of frontal regions in older adults signals the need to maintain top-down control over task performance in order to achieve a performance level comparable with that of younger individuals due to degradation of the primary task network (Davis et al., 2008; Goh and Park, 2009). An extensive ERP literature has suggested that the age-related anterior shift in the topography of the P300 also arises from compensatory prefrontal recruitment (e.g., Fabiani et al., 1998; West et al., 2010) but it has not been possible to properly test this theory until now. Specifically, ERP studies have shown that younger participants habituate more quickly to target and distractor stimuli on the oddball task, reflected in a reduction in P300 amplitude over frontal sites (Fabiani et al., 1995; Richardson et al., 2011; West et al., 2010). Several authors have consequently proposed that where younger participants are able to rapidly establish a strong mental representation of task stimuli and delegate stimulus processing to posterior attention regions, elderly participants continue to rely on anterior control regions to maintain task performance at a comparable level. Our finding that the elderly group showed increased recruitment of right dorsolateral prefrontal cortex during P3b processing and left inferior prefrontal cortex during P3a processing provides broad support for the proposal that P300 age effects arise from an increased reliance on higher level control regions to support task performance. Equally, our finding that young participants showed increased recruitment of inferior parietal cortex conforms to the proposal that they are more reliant on posterior brain regions.

The lateralization of the frontal group differences maps on to a general trend that has emerged from functional imaging studies that the right hemisphere dominates target processing while the left hemisphere is more active during distractor processing (Eichele et al., 2005; Madden et al., 2007). The right dorsolateral prefrontal cortex is a key supramodal attentional control region commonly engaged during the detection and response to salient, goal-relevant stimuli, and activation levels within this region have been previously shown to correlate with response times (Bledowski et al., 2004; Eichele et al., 2005; Kirino et al., 2000; Solbakk et al., 2008). The left inferior frontal cortex has also been heavily implicated in cognitive control, specifically in response inhibition and aspects of working memory (Aron and Poldrack, 2005; McDermott et al., 2003), and forms part of a broader attentional control network that also includes the cingulate cortex and putamen (Tekin and Cummings, 2002), both of which showed greater activity for the elderly group.

The posterior anterior shift in aging (PASA; Davis et al., 2008) model postulates that older adults must rely on frontal mechanisms to support task performance in order to compensate for diminished function within posterior perceptual processing regions. It is noteworthy therefore that the elderly group in this study had significantly smaller occipital P1 and P2 amplitudes relative to the young group and that the young group showed significantly increased P3a activity in right inferior parietal cortex, a region that has been associated with visual attention switching and novelty detection (Bledowski et al., 2004). In fact, the literature regarding the effects of advancing age on early visual processing components such as P1 and N1 is somewhat inconsistent, with some studies reporting amplitude increases and others decreases, and this is likely due to the fact that the age-related effects vary depending on the task demands of a given study (e.g., see De Sanctis et al., 2008;

Falkenstein et al., 2006 for discussion). For example, 2 recent studies, 1 using a task that exerted no cognitive demand at all (De Sanctis et al., 2008) and another using a Sternberg memory task (Finnigan et al., 2011) reported that their elderly participants had significantly delayed N1 peak latencies but larger amplitudes. Source analyses, reported in these same studies, suggested that these N1 differences arose in part from increased recruitment of prefrontal cortex and reduced hemispheric specialization in occipitoparietal cortex. Unfortunately, previous ERP aging studies using the visual oddball task have not reported results for P1 and N1 components. Although the specific results vary across studies depending on the paradigms used, the accumulated evidence from visual evoked potentials, including that of the present study, points to age-related inefficiencies at the earliest stages of perceptual processing but also suggests that compensatory recruitment of additional brain regions may begin at processing stages that precede those of the P300. While our analyses were focused specifically on the P3a and P3b our data are broadly consistent the posterior anterior shift in aging model and suggest that the increased frontal engagement of the elderly group may arise in part from a need to overcome inefficient early perceptual processing of task stimuli. Future studies with larger sample sizes would be desirable to explore the potential relationship between early visual processing deficits and the EEG/fMRI markers identified here.

There were also significant age-related differences in hippocampus activation associated with P3a and P3b with the elderly group showing greater engagement of right hippocampus in both cases. Human lesion studies suggest that the hippocampus is particularly important for the generation of the frontal component of the P3a (Knight, 1996) but depth electrode recordings and functional imaging (Eichele et al., 2005; McCarthy et al., 1989) have indicated that the hippocampus also contributes to the P3b. The hippocampus is commonly recruited in tasks that require deviance detection and involuntary attentional orienting and performs key functions subserving executive control and memory (Knight, 1996; Yamaguchi et al., 2004). The hippocampus undergoes significant volumetric reductions with age that are correlated to memory function and cross-sectional research suggests that the left hippocampus may be particularly vulnerable (Ystad et al., 2009). This structure is also 1 of the earliest brain regions to exhibit atrophy in mild cognitive impairment and in the early stages of Alzheimer's disease (AD; Convit et al., 1997). Further research is therefore warranted to investigate the extent to which these combined P300/hippocampal functional markers can contribute to the earlier detection of dementia.

This study represents the first effort to address the intracranial origins of P300 aging effects using concurrent fMRI and EEG analyses and a number of methodological issues should be taken into consideration. First, the sample size used, although comparable with that of other EEG/fMRI studies, is relatively small and the oddball performance data suggest our older group may have been relatively high-functioning. The sample size also meant that we were unable to contribute to the understanding of the functional relevance of the additional anterior recruitment we observed in older subjects. For example, Fabiani et al. (1998) and West et al. (2010) found that elderly participants with larger frontal P300s performed worse on neuropsychological tests of frontal function. This finding is at odds with several neuroimaging studies that have reported positive relationships between frontal activity and cognitive performance in aging and further work will be required to address this issue. Second, while the conventional fMRI results were subjected to corrections for multiple comparisons, an uncorrected threshold of $p < 0.001$ was used for the EEG/fMRI data fusion. This approach is consistent with a majority of EEG/fMRI studies (e.g., Ben-Simon et al., 2008; Debettencourt et al., 2011; Eichele et al., 2005; Karch et al., 2010; Novitskiy et al., 2011) but some have reported significant results using corrected thresholds (Huster et al., 2011; Mantini et al., 2009) and so our results will require further replication. Third, our analyses focused specifically on P300 amplitude but latency has also demonstrated sensitivity to aging and would also warrant investigation in future studies. Fourth, our results are based on smoothed single-trial ERP information and therefore represent tonic relationships between fMRI and ERP measures. Further work is required to investigate the influence of different approaches to single-trial ERP measurement (e.g., smoothed vs. unsmoothed) on the outcome of fusion analyses. Finally, a limitation of the EEG/fMRI method is that it is not possible to determine whether the highlighted brain regions directly contribute to the generation of the P300 or if they were identified because they modulate regions that are direct generators.

In conclusion we report the first simultaneous EEG/fMRI study of aging that seeks to explore the intracranial origins of 1 of the most consistently reported electrophysiological markers of aging—the P300. Our results highlight significant age differences in brain regions that have been repeatedly identified as generators of the P300 with the older group showing significantly greater recruitment of frontal and temporal structures. The combination of sophisticated temporal and spatial information from concurrent EEG and fMRI has the potential to greatly enhance the utility of the P300 as a biomarker for aging and neuropsychiatric disorders.

Disclosure statement

The authors report no conflicts of interest.

Participants gave written informed consent prior to the study which was approved by the Trinity College Dublin School of Psychology Ethics Committee.

Acknowledgements

This work was supported by funding from the Glaxo-SmithKline/Trinity College Institute of Neuroscience Research Consortium on Neurodegeneration. R.G. O'Connell and J.H. Balsters are currently supported by fellowships from the Irish Research Council for Science Engineering and Technology (IRCSET).

Appendix A. Supplementary data

Supplementary data associated with this article can be found, in the online version, at doi:10.1016/j.neurobiolaging.2011.12.021.

References

Aguirre, G.K., Zarahn, E., D'Esposito, M., 1998. The variability of human, BOLD hemodynamic responses. Neuroimage 8, 360–369.

Allen, P.J., Josephs, O., Turner, R., 2000. A method for removing imaging artifact from continuous EEG recorded during functional MRI. Neuroimage 12, 230–239.

Allen, P.J., Polizzi, G., Krakow, K., Fish, D.R., Lemieux, L., 1998. Identification of EEG events in the MR scanner: the problem of pulse artifact and a method for its subtraction. Neuroimage 8, 229–239.

Andersson, J.L., Hutton, C., Ashburner, J., Turner, R., Friston, K., 2001. Modeling geometric deformations in EPI time series. Neuroimage 13, 903–919.

Aron, A.R., Poldrack, R.A., 2005. The cognitive neuroscience of response inhibition: relevance for genetic research in attention-deficit/hyperactivity disorder. Biol. Psychiatry 57, 1285–1292.

Ashburner, J., Friston, K.J., 2005. Unified segmentation. Neuroimage 26, 839–851.

Balsters, J.H., Ramnani, N., 2008. Symbolic representations of action in the human cerebellum. Neuroimage 43, 388–398.

Ben-Simon, E., Podlipsky, I., Arieli, A., Zhdanov, A., Hendler, T., 2008. Never resting brain: simultaneous representation of two alpha related processes in humans. PLoS One 3, e3984.

Bledowski, C., Prvulovic, D., Goebel, R., Zanella, F.E., Linden, D.E., 2004. Attentional systems in target and distractor processing: a combined ERP and fMRI study. Neuroimage 22, 530–540.

Cabeza, R., Anderson, N.D., Locantore, J.K., McIntosh, A.R., 2002. Aging gracefully: compensatory brain activity in high-performing older adults. Neuroimage 17, 1394–1402.

Convit, A., De Leon, M.J., Tarshish, C., De Santi, S., Tsui, W., Rusinek, H., George, A., 1997. Specific hippocampal volume reductions in individuals at risk for Alzheimer's disease. Neurobiol. Aging 18, 131–138.

D'Esposito, M., Deouell, L.Y., Gazzaley, A., 2003. Alterations in the BOLD fMRI signal with ageing and disease: a challenge for neuroimaging. Nat. Rev. Neurosci. 4, 863–872.

Davis, S.W., Dennis, N.A., Daselaar, S.M., Fleck, M.S., Cabeza, R., 2008. Que PASA? The posterior-anterior shift in aging. Cereb. Cortex 18, 1201–1209.

De Sanctis, P., Katz, R., Wylie, G.R., Sehatpour, P., Alexopoulos, G.S., Foxe, J.J., 2008. Enhanced and bilateralized visual sensory processing in the ventral stream may be a feature of normal aging. Neurobiol. Aging 29, 1576–1586.

Debener, S., Mullinger, K.J., Niazy, R.K., Bowtell, R.W., 2008. Properties of the ballistocardiogram artefact as revealed by EEG recordings at 1.5, 3 and 7 T static magnetic field strength. Int. J. Psychophysiol. 67, 189–199.

Debener, S., Strobel, A., Sorger, B., Peters, J., Kranczioch, C., Engel, A.K., Goebel, R., 2007. Improved quality of auditory event-related potentials recorded simultaneously with 3-T fMRI: removal of the ballistocardiogram artefact. Neuroimage 34, 587–597.

Debener, S., Ullsperger, M., Siegel, M., Fiehler, K., von Cramon, D.Y., Engel, A.K., 2005. Trial-by-trial coupling of concurrent electroencephalogram and functional magnetic resonance imaging identifies the dynamics of performance monitoring. J. Neurosci. 25, 11730–11737.

Debettencourt, M., Goldman, R., Brown, T., Sajda, P., 2011. Adaptive thresholding for improving sensitivity in single-trial simultaneous EEG/FMRI. Front. Psychol. 2, 91.

Dockree, P.M., Kelly, S.P., Robertson, I.H., Reilly, R.B., Foxe, J.J., 2005. Neurophysiological markers of alert responding during goal-directed behavior: a high-density electrical mapping study. Neuroimage 27, 587–601.

Donchin, E., 1981. Presidential address, 1980. Surprise!. . .Surprise? Psychophysiology 18, 493–513.

Eichele, T., Specht, K., Moosmann, M., Jongsma, M.L., Quiroga, R.Q., Nordby, H., Hugdahl, K., 2005. Assessing the spatiotemporal evolution of neuronal activation with single-trial event-related potentials and functional MRI. Proc. Natl. Acad. Sci. U. S. A. 102, 17798–17803.

Fabiani, M., Friedman, D., 1995. Changes in brain activity patterns in aging: The novelty oddball. Psychophysiology 32, 579–594.

Fabiani, M., Friedman, D., Cheng, J.C., 1998. Individual differences in P3 scalp distribution in older adults, and their relationship to frontal lobe function. Psychophysiology 35, 698–708.

Falkenstein, M., Yordanova, J., Kolev, V., 2006. Effects of aging on slowing of motor-response generation. Int. J. Psychophysiol. 59, 22–29.

Finnigan, S., O'Connell, R.G., Cummins, T.D., Broughton, M., Robertson, I.H., 2011. ERP measures indicate both attention and working memory encoding decrements in aging. Psychophysiology 48, 601–611.

Fjell, A.M., Walhovd, K.B., 2004. Life-span changes in P3a. Psychophysiology 41, 575–583.

Friedman, D., 2003. Cognition and aging: a highly selective overview of event-related potential (ERP) data. J. Clin. Exp. Neuropsychol. 25, 702–720.

Friston, K.J., Frith, C.D., Frackowiak, R.S., Turner, R., 1995a. Characterizing dynamic brain responses with fMRI: a multivariate approach. Neuroimage 2, 166–172.

Friston, K.J., Frith, C.D., Turner, R., Frackowiak, R.S., 1995b. Characterizing evoked hemodynamics with fMRI. Neuroimage 2, 157–165.

Goh, J.O., Park, D.C., 2009. Neuroplasticity and cognitive aging: The scaffolding theory of aging and cognition. Restor. Neurol. Neurosci. 27, 391–403.

Gunning-Dixon, F.M., Raz, N., 2003. Neuroanatomical correlates of selected executive functions in middle-aged and older adults: a prospective MRI study. Neuropsychologia 41, 1929–1941.

Halgren, E., Baudena, P., Clarke, J.M., Heit, G., Marinkovic, K., Devaux, B., Vignal, J.P., Biraben, A., 1995. Intracerebral potentials to rare target and distractor auditory and visual stimuli. II. Medial, lateral and posterior temporal lobe. Electroencephalogr. Clin. Neurophysiol. 94, 229–250.

Handwerker, D.A., Ollinger, J.M., D'Esposito, M., 2004. Variation of BOLD hemodynamic responses across subjects and brain regions and their effects on statistical analyses. Neuroimage 21, 1639–1651.

Huster, R.J., Eichele, T., Enriquez-Geppert, S., Wollbrink, A., Kugel, H., Konrad, C., Pantev, C., 2011. Multimodal imaging of functional networks and event-related potentials in performance monitoring. Neuroimage 56, 1588–1597.

Hutton, C., Bork, A., Josephs, O., Deichmann, R., Ashburner, J., Turner, R., 2002. Image distortion correction in fMRI: A quantitative evaluation. Neuroimage 16, 217–240.

Iannetti, G.D., Niazy, R.K., Wise, R.G., Jezzard, P., Brooks, J.C., Zambreanu, L., Vennart, W., Matthews, P.M., Tracey, I., 2005. Simultaneous recording of laser-evoked brain potentials and continuous, high-field functional magnetic resonance imaging in humans. Neuroimage 28, 708–719.

Kannurpatti, S.S., Motes, M.A., Rypma, B., Biswal, B.B., 2010. Neural and vascular variability and the fMRI-BOLD response in normal aging. Magn. Reson. Imaging 28, 466–476.

Karch, S., Feuerecker, R., Leicht, G., Meindl, T., Hantschk, I., Kirsch, V., Ertl, M., Lutz, J., Pogarell, O., Mulert, C., 2010. Separating distinct aspects of the voluntary selection between response alternatives: N2- and P3-related BOLD responses. Neuroimage 51, 356–364.

Kelly, A.M., Garavan, H., 2005. Human functional neuroimaging of brain changes associated with practice. Cereb. Cortex 15, 1089–1102.

Kiehl, K.A., Laurens, K.R., Duty, T.L., Forster, B.B., Liddle, P.F., 2001. Neural sources involved in auditory target detection and novelty processing: an event-related fMRI study. Psychophysiology 38, 133–142.

Kirino, E., Belger, A., Goldman-Rakic, P., McCarthy, G., 2000. Prefrontal activation evoked by infrequent target and novel stimuli in a visual target detection task: an event-related functional magnetic resonance imaging study. J. Neurosci. 20, 6612–6618.

Knight, R., 1996. Contribution of human hippocampal region to novelty detection. Nature 383, 256–259.

Linden, D.E., 2005. The p300: where in the brain is it produced and what does it tell us? Neuroscientist 11, 563–576.

Logothetis, N.K., Pauls, J., Augath, M., Trinath, T., Oeltermann, A., 2001. Neurophysiological investigation of the basis of the fMRI signal. Nature 412, 150–157.

Madden, D.J., Spaniol, J., Whiting, W.L., Bucur, B., Provenzale, J.M., Cabeza, R., White, L.E., Huettel, S.A., 2007. Adult age differences in the functional neuroanatomy of visual attention: a combined fMRI and DTI study. Neurobiol. Aging 28, 459–476.

Madden, D.J., Whiting, W.L., Provenzale, J.M., Huettel, S.A., 2004. Age-related changes in neural activity during visual target detection measured by fMRI. Cereb. Cortex 14, 143–155.

Mantini, D., Corbetta, M., Perrucci, M.G., Romani, G.L., Del Gratta, C., 2009. Large-scale brain networks account for sustained and transient activity during target detection. Neuroimage 44, 265–274.

McCarthy, G., Wood, C.C., Williamson, P.D., Spencer, D.D., 1989. Task-dependent field potentials in human hippocampal formation. J. Neurosci. 9, 4253–4268.

McDermott, K.B., Petersen, S.E., Watson, J.M., Ojemann, J.G., 2003. A procedure for identifying regions preferentially activated by attention to semantic and phonological relations using functional magnetic resonance imaging. Neuropsychologia 41, 293–303.

Mullinger, K.J., Morgan, P.S., Bowtell, R.W., 2008. Improved artifact correction for combined electroencephalography/functional MRI by means of synchronization and use of vectorcardiogram recordings. J. Magn. Reson. Imaging 27, 607–616.

Nieuwenhuis, S., Aston-Jones, G., Cohen, J.D., 2005. Decision making, the P3, and the locus coeruleus-norepinephrine system. Psychol. Bull. 131, 510–532.

Novitskiy, N., Ramautar, J.R., Vanderperren, K., De Vos, M., Mennes, M., Mijovic, B., Vanrumste, B., Stiers, P., Van den Bergh, B., Lagae, L., Sunaert, S., Van Huffel, S., Wagemans, J., 2011. The BOLD correlates of the visual P1 and N1 in single-trial analysis of simultaneous EEG-fMRI recordings during a spatial detection task. Neuroimage 54, 824–835.

Polich, J., 1997. On the relationship between EEG and P300: individual differences, aging, and ultradian rhythms. Int. J. Psychophysiol. 26, 299–317.

Polich, J., 2007. Updating P300: an integrative theory of P3a and P3b. Clin. Neurophysiol. 118, 2128–2148.

Polich, J., Criado, J.R., 2006. Neuropsychology and neuropharmacology of P3a and P3b. Int. J. Psychophysiol. 60, 172–185.

Quian Quiroga, R., Garcia, H., 2003. Single-trial event-related potentials with wavelet denoising. Clin. Neurophysiol. 114, 376–390.

Raz, N., 2000. Aging of the brain and its impact on cognitive performance: Integration of structural and functional findings, in: Craik, F.I.M., Salthouse, T.A. (Eds.), Handbook of Aging and Cognition, second ed. Erlbaum, Mahwah, NJ, pp. 1–90.

Raz, N., Lindenberger, U., Rodrigue, K.M., Kennedy, K.M., Head, D., Williamson, A., Dahle, C., Gerstorf, D., Acker, J.D., 2005. Regional brain changes in aging healthy adults: general trends, individual differences and modifiers. Cereb. Cortex 15, 1676–1689.

Richardson, C., Bucks, R.S., Hogan, A.M., 2011. Effects of aging on habituation to novelty: An ERP study. Int. J. Psychophysiol. 79, 97–105.

Rossini, P.M., Rossi, S., Babiloni, C., Polich, J., 2007. Clinical neurophysiology of aging brain: from normal aging to neurodegeneration. Prog. Neurobiol. 83, 375–400.

Snyder, E., Hillyard, S.A., 1976. Long-latency evoked potentials to irrelevant, deviant stimuli. Behav. Biol. 16, 319–331.

Solbakk, A.K., Fuhrmann Alpert, G., Furst, A.J., Hale, L.A., Oga, T., Chetty, S., Pickard, N., Knight, R.T., 2008. Altered prefrontal function with aging: insights into age-associated performance decline. Brain Res. 1232, 30–47.

Strobel, A., Debener, S., Sorger, B., Peters, J.C., Kranczioch, C., Hoechstetter, K., Engel, A.K., Brocke, B., Goebel, R., 2008. Novelty and target processing during an auditory novelty oddball: a simultaneous event-related potential and functional magnetic resonance imaging study. Neuroimage 40, 869–883.

Sutton, S., Braren, M., Zubin, J., John, E.R., 1965. Evoked-potential correlates of stimulus uncertainty. Science 150, 1187–1188.

Tekin, S., Cummings, J.L., 2002. Frontal-subcortical neuronal circuits and clinical neuropsychiatry: an update. J. Psychosom. Res. 53, 647–654.

Verleger, R., 2008. P3b: towards some decision about memory. Clin. Neurophysiol. 119, 968–970.

Warbrick, T., Mobascher, A., Brinkmeyer, J., Musso, F., Richter, N., Stoecker, T., Fink, G.R., Shah, N.J., Winterer, G., 2009. Single-trial P3 amplitude and latency informed event-related fMRI models yield different BOLD response patterns to a target detection task. Neuroimage 47, 1532–1544.

West, R., Schwarb, H., Johnson, B.N., 2010. The influence of age and individual differences in executive function on stimulus processing in the oddball task. Cortex 46, 550–563.

Wylie, G.R., Javitt, D.C., Foxe, J.J., 2003. Task switching: a high-density electrical mapping study. Neuroimage 20, 2322–2342.

Yamaguchi, S., Hale, L.A., D'Esposito, M., Knight, R.T., 2004. Rapid prefrontal-hippocampal habituation to novel events. J. Neurosci. 24, 5356–5363.

Ystad, M.A., Lundervold, A.J., Wehling, E., Espeseth, T., Rootwelt, H., Westlye, L.T., Andersson, M., Adolfsdottir, S., Geitung, J.T., Fjell, A.M., Reinvang, I., Lundervold, A., 2009. Hippocampal volumes are important predictors for memory function in elderly women. BMC Med. Imaging 9, 17.